Sedimentologika

Research article

Constraining the formation conditions of modern pisoids at Ore Lake, Michigan

Ryleigh Landstra*, Ian Winkelstern

Department of Geology, Grand Valley State University, 1 Campus Dr., Allendale, Michigan, United States

*corresponding author: Ryleigh Landstra (ryleighl@umich.edu)

doi: 10.57035/journals/sdk.2023.e11.1179

Editors: Carolina N. Keim and Latisha Brengman
Reviewers: Philip Fralick and one anonymous reviewer
Copyediting, layout and production: Romain Vaucher, Thomas J.H. Dodd and Gabriel Bertolini

Submitted: 01.05.2023
Accepted: 19.09.2023
Published: 20.11.2023

Abstract | Large concentrically laminated carbonate grains (here referred to as pisoids) have been observed sporadically throughout the geological record and in modern environments. Explanations for how these grains form have varied widely in different settings, although microbial effects are often involved. In Ore Lake, a ~1 km^2 flow-through lake in southeast Michigan, one to four centimeter oblong calcite pisoids are observed in both lake bottom shallows and mounded as a small spit near the primary outflow. In section mm-scale light and more porous along with and dark and more dense concentric laminations are apparent. Here we use field observations, petrography, water chemistry, and stable isotopes to understand their formation. Measurements of pisoid calcite $\delta^{18}O$ and lake water $\delta^{18}O$ indicate that precipitation occurs in waters between roughly 19 – 28°C. These warm temperatures imply that pisoid growth happens almost entirely within the summer, contrary to prior work that suggested wintertime precipitation was important. Pisoid $\delta^{18}O$ values largely overlap with coexisting lake bivalve values, suggesting that pisoid precipitation is in equilibrium. In contrast, pisoid $\delta^{13}C$ is as much as 8 ‰ more positive than bivalve $\delta^{13}C$ due to photosynthetic effects. We propose that the laminations in these pisoids arise from different rates of formation within the warm months, rather than large seasonal differences. A decline in lake alkalinity beginning in late spring likely coincides with more rapid growth, with slower growth mediated by cyanobacteria continuing through the summer. This range of observations enables the use of Ore Lake as a potential model for understanding pisoid formation throughout the geological record.

Lay summary | Here, we investigate how unique, concentrically layered grains ("pisoids") are forming in a small inland lake in Michigan, USA. We use field observations, thin sections, and measurements of grain and water composition to learn about their formation. We find that the pisoids form in close association with local cyanobacteria during the warm months, which are likely moved around as they grow. Studies that examine how pisoliths form today can inform how we interpret them in ancient geological deposits.

Keywords: Pisoids, Stable isotopes, Lacustrine, Carbonate, Modern analogue

1. Introduction

Carbonate precipitation in association with cyanobacteria is common in ancient and modern settings, but the character of the precipitate and the precise details of how it forms are highly variable (Pedley, 1990; Benzerara et al., 2014; Chafetz et al., 2018). The morphology of microbial carbonates can differ greatly; such structures include tufa, travertine, stromatolites, oncoids, spherulites, microbialites, and pisoids or pisoliths (Chafetz & Meredith,1983; Folk & Chafetz, 1983; Riding, 1983; Rivera & Sumner, 2014; Chafetz 2018). Settings where cyanobacteria-driven precipitation occurs are thought to include nearly all places where carbonates form, including hot springs and geysers (Chafetz, 2018), shallow marine environments (Reid et al., 2000), and freshwater environments such as lakes (Andrews & Trewin, 2014; Chagas et al., 2016) and streams (Merz-Preiß & Riding, 1999; Andrews, 2006), from the modern and Holocene through the Archean (e.g., Rivera & Sumner, 2014).

Concentrically laminated carbonates (including microbialites) in particular have attracted interest for decades (e.g., Irion & Müller, 1968; Dunham, 1969; Dahanayake, 1977;

This is an open access article under the terms of the Creative Commons Attribution License (CC-BY) © 2023 The Authors

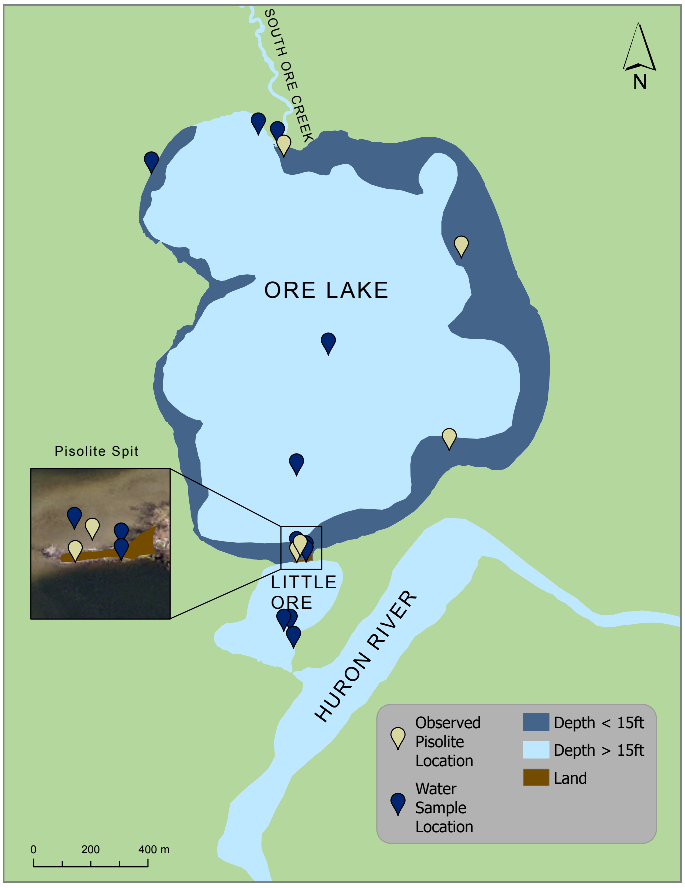

Figure 1 | Map of water and carbonate sample locations within Ore Lake, Michigan, USA.

Risacher & Eugster, 1979). Broadly defined, these concentric structures larger than ooids also have been described from modern settings and throughout the geologic record (e.g., Monty & Mas, 1981; Maliva, 2000; Rivera & Sumner, 2014). Concentric laminations are known to form from both biotic and abiotic factors. In some cases, vadose zone precipitation (Dunham, 1969) and/or hypersaline precipitation (Esteban & Prey, 1983) are thought to create concentric laminations abiotically. However, cyanobacteria likely play a role in most concentric carbonate formation processes (e.g., Barth & Chafetz, 2015; Mors et al., 2022). For example, bacteria can help to instigate precipitation that proceeds in part abiotically (Chafetz & Meredith, 1983; Barth & Chafetz, 2015), or play a role in precipitation throughout the growth of concentric structures (Chafetz et al., 2018). Indeed, the presence of amino acids and extracellular polymeric substances (even when the organisms were no longer living), are enough to induce carbonate precipitation in concentric patterns (Braissant et al., 2007). The common assumption of microbially induced precipitation, in general, is that given the 'right' conditions (e.g., particular saturation states, temperatures, and alkalinity), cyanobacteria can promote carbonate precipitation by altering local water chemistry through photosynthetic processes (Merz-Preiß & Riding, 1999; Braissant et al., 2007; Müller et al., 2016; Chafetz et al., 2017; Turchyn, 2021; Shiraishi et al., 2022).

This paper focuses on freshwater pisoids in a humid continental setting at Ore Lake, Michigan, USA (Figure 1), an inland, temperate marl lake (Binkley et al., 1980). The definitions of 'pisoids' differ in the literature; here we use the term to describe oblong to circular, concentrically banded, tufa-like structures one to four centimeters in diameter (Figure 2). At Ore Lake, these calcareous forms have been found to have both skeletal (gastropods and bivalves) and non-skeletal nuclei. Nearly all samples display concentric banding around the center. The samples observed in this study are all thought to be modern. Ore Lake has long been noted for carbonate deposition in the form of marl (Pollock, 1919), pisoids (Jones & Wilkinson, 1978), and carbonate-cemented beachrock (Binkley et al., 1980). Cyanobacteria (previously known as 'blue-green algae') are seasonally abundant in Ore Lake (Parker & Kohlhepp, 2017) and are understood to play a role in local carbonate formation for over 100 years (Pollock, 1919).

Jones & Wilkinson (1978) concluded that the Ore Lake pisoids likely remained in place during precipitation, based on the general observation of flattened bases of their samples. They determined that this flattening represented an area of the pisoid that remained in contact with the lake bottom sediment. While precipitation favors the side of the structure that is most available for photosynthesis, they noted that precipitation must occur on all sides of the pisoids to obtain the concentric banding observed. Jones & Wilkinson (1978) also noted that clear dark and light banding within the pisoids was due to variations in porosity (Figure 3), with porous layers containing more filamental structures. They concluded that this difference in layer composition indicated year-round precipitation, with photosynthesis only contributing to carbonate precipitation during warmer months and a nearly equivalent amount of abiotic precipitation occurring during the winter (Jones & Wilkinson, 1978). In this study, we seek to reassess whether such substantial carbonate precipitation during winter months (when our observations indicate the lake surface is often partially frozen) is likely.

This study aims to broadly refine the conditions of carbonate precipitation in Ore Lake, particularly investigating pisoid formation and the possibility of winter precipitation (perhaps abiotic). We use stable isotope data to constrain the water chemistry and temperature at the time of pisoid formation. We also assess the location of pisoid formation and transportation within the lake; field observations indicate that Ore Lake has sufficient flow for grains in shallow areas to be transported towards the lake outflow in the south (Figure 1). This study evaluates how these findings may be relevant for studies of similar concentric grains throughout the geological record.

2. Methods

2.1. Sampling

Water samples were collected from Ore Lake over a visit in October 2016, one visit in February 2017, and three visits between July and October 2021. Single-visit sampling also

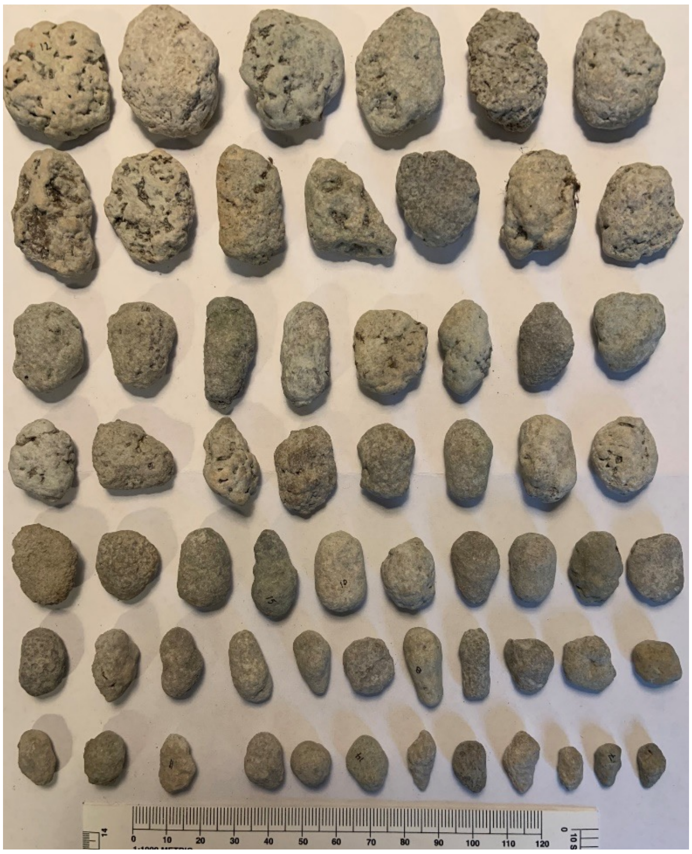

Figure 2 | A range of complete pisoids that were sampled from Ore Lake. Scale bar in millimeters.

included the connecting Huron River, four nearby lakes (Zukey, Bass, Bishop, and Lime), South Ore Creek (which flows into Ore Lake), and one sample from a nearby park faucet located southeast of Ore Lake, which was sampled to represent local groundwater (Supplemental Figure 1). Carbonates analyzed here were collected from Ore Lake in July 2021 from the northern shore and a spit on the southern shore (Figures 1 and 4).

Water sampling was conducted using sterile 10mL syringes, welded syringe filters, and 5mL glass vials. These samples were collected from surface waters using a boat as well as from the shore, depending on the trip and the targeted areas. Alkalinity testing was conducted using the titration method, where total alkalinity was expressed in mg/L (Lamotte 4491-DR-01 Water Quality Testing Kit). In-the-field testing of water pH, conductivity (μs), and total dissolved solids (ppm) was conducted using a water quality meter with a +/-1 % accuracy.

2.2. Stable isotope methods

$\delta^{18}O$ and δD of water samples collected in 2021 were measured at the Iowa State University Stable Isotope Lab (ISU). Older samples from 2016 and 2017 were measured at the University of Michigan (U of M). Both sample sets were measured using a Picarro L2130-i Isotopic Liquid Water Analyzer, with an autosampler and the ChemCorrect software. For ISU samples, the final three injections (of six total) were used to calculate mean isotopic values to account for memory effects. For U of M samples, the last

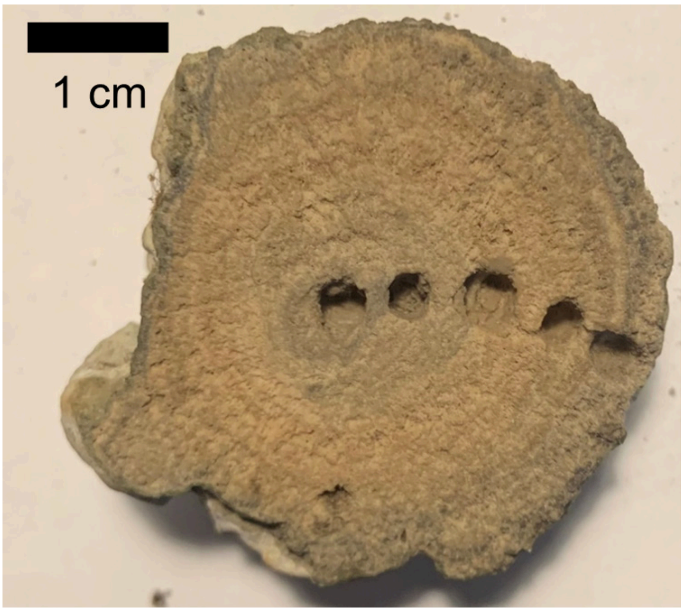

Figure 3 | Cross-section of pisoid sample SP1, which was sub-sampled for stable isotopes (small holes). Note circular concentric layering.

four analyses of nine measurements were used. In both labs, USGS 47 and USGS 48 reference standards (USGS, 2023) were used for regression-based isotopic corrections and to assign the data to the appropriate isotopic scale in which at least one standard was used for every five samples. The combined uncertainty (analytical uncertainty and average correction factor) for water $\delta^{18}O$ ($\delta^{18}O_{water}$) is ± 0.1 ‰ (VSMOW) and for δD is ± 0.5 ‰ (VSMOW).

Carbonate $\delta^{18}O$ and $\delta^{13}C$ of sixteen pisoids and four shells identified at genus level (three *Dreissena* and and one *Corbicula*) were measured at the U of M Stable Isotope Lab relative to internal standards and the Vienna Peedee Belemnite standard (VPDB). Four of these pisoids were subsampled in multiple places across apparent growth laminae (Figure 3). The subsamples were obtained using a handheld Dremel tool, which unfortunately was too large to enable reliably discrete sampling from pisoid layers (that is, several subsamples include some portion of a light and darker layer). The other twelve pisoids had one sample taken from the outer surface of each, which was completed after abrading away the outermost ~1 – 2 mm of carbonate and debris. The bivalves were sampled from just one location along the outside of the shell. All samples were measured for both $\delta^{18}O$ and $\delta^{13}C$ using a Kiel IV automated preparation device coupled to a Thermo Scientific MAT 253 mass spectrometer at the University of Michigan Stable Isotope Laboratory. The analytical precision was greater than 0.1 ‰.

Formation temperature was calculated from carbonate $\delta^{18}O$ data using mineral-specific fractionation factors. For calcite pisoids we used Kim & O'Neil (1997). For aragonite shells we used Grossman & Ku (1986). For all samples we input a $\delta^{18}O_{water}$ value of -5.6 ‰. This value is the mean of all $\delta^{18}O_{water}$ measurements within Ore Lake, excluding the single sample taken during winter. The effect of

Figure 4 | Field photo of surficial sediments on the spit at the southern end of Ore Lake (see map in Figure 1). The very coarse-grained sediment here is dominated by disarticulated quagga mussel shells, complete pisoids, and pisoid fragments.

changing the $\delta^{18}O_{water}$ value used for calculating temperatures (including the winter $\delta^{18}O_{water}$ value, for example) is discussed below. We treat these calculations as an estimate of temperature and not as an exact measurement. This is because $\delta^{18}O_{water}$ certainly varies through time and within the lake (although the data suggest that lake $\delta^{18}O_{water}$ values are relatively constant across summer and fall; see results).

3. Geochemical results

3.1. Field observations

We located pisoids in four locations in Ore Lake: partially buried within sediment at the northern shore near where South Ore Creek enters Ore Lake, two locations along the east side of the lake, and as part of an elevated spit at the southern end (Sample Location map). This ~60 m spit structure is made up primarily of mollusk shells, coarse carbonate sand, fragmented pisoids, and complete pisoids (Figure 4). The spit juts into the water where Ore Lake drains into the much smaller (~0.05 km^2) Little Ore Lake and subsequently the Huron River to the south, helping to separate the two lakes. The composition and morphology of the spit, as well as the north-to-south current in Ore Lake, suggest that it formed from apparent changes in shoreline currents and/or wave energy at this drainage point.

The pisoids collected from the northern shore of the lake (where South Ore Creek drains into it) were located < 5 m from shore and were sampled from under approximately 25 – 75 mm of sand. The pisoids were much less abundant than in the area in and around the southern spit (Figure 1). The burial of these samples may have been due to high lake levels (and creek discharge) occurring at the time of collection. In addition, pisoids were located in two areas in the eastern part of the lake, where a shallow (< 3 m) shelf extends ~200 m from shore. These were observed and sampled in water ~2 m and ~0.75 m deep.

3.2. Alkalinity

The alkalinity of lake water indicates the availability of bicarbonate ions for uptake during photosynthesis, which in turn increases the likelihood of carbonate precipitation by cyanobacteria or algae (e.g., Merz, 1992). As far as we have observed, Ore Lake is locally unique in forming pisoids and/or significant microbialite formation. Enhanced carbonate precipitation in Ore Lake is therefore consistent with elevated alkalinity relative to nearby lakes. Our measurements of Ore Lake alkalinity range from 136 to 164 ppm $CaCO_3$ (Table 1). Measurements from nearby Bishop, Zukey, and Bass lakes range from 88 to 126 ppm $CaCO_3$ (Table 1). Water samples taken from South Ore Creek showed the greatest surface water alkalinity concentration, ranging from 156 – 168 ppm $CaCO_3$. As presented in Supplemental 2, there is a decline in surface water alkalinity from the north to the south, with higher alkalinity South Ore Creek waters mixing with other sources (including groundwater) within Ore Lake (Figure 1). As such, the northernmost sample location within the lake also had the highest alkalinity within the lake. The potential relationship between spatial variability of lake surface alkalinity and pisoid formation is discussed below.

Sample	Location	Sampling Date	Latitude / Longitude	$\delta^{18}O$ (VSMOW)	δD (VSMOW)	Alk. (mg/L)	pH	Cond. (μs)	TDS (ppm)
OLWI	South Ore Creek	7/17/2021	42.49770N 83.80210W	-5.87	-43.06	156	no data	no data	no data
OLW2	Huron River	7/17/2021	42.47500N 83.78850W	no data	no data	144	no data	no data	no data
OLW3	Ore Lake (shoal)	7/17/2021	42.47580N 83.79660W	-5.75	-43.55	136	no data	no data	no data
OLW4	Ore Lake (middle)	7/17/2021	42.47780N 83.79690W	-5.77	-43.45	148	no data	no data	no data
BILW24	Bishop Lake	7/17/2021	42.50260N 83.84260W	-2.65	-29.62	88	no data	no data	no data
ZLW25	Zukey Lake	9/4/2021	42.46310N 83.84690W	-4.25	-32.8	124	no data	no data	no data
BALW26	Bass Lake	9/4/2021	42.44900N 83.85680W	-4.56	-35.09	128	no data	no data	no data
OLW8	South Ore Creek	9/4/2021	42.49040N 83.79860W	-5.25	-38.81	no data	no data	no data	no data
OLW9	Little Ore Lake (south)	9/4/2021	42.47380N 83.7969W	-5.19	-38.79	144	no data	no data	no data
OLW10	Well Water Sample	10/2/2021	42.4752N 83.7825W	no data	no data	212	8.28	661.4	447.3
OLW11	Little Ore Lake (middle)	10/2/2021	42.47420N 83.79710W	-5.93	-43.6	140	8.91	778.6	533.8
OLW12	Ore Lake (shoal)	10/2/2021	42.47590N 83.79660W	-5.52	-41.3	140	8.93	777.9	535.1
OLW13	Ore Lake (middle)	10/2/2021	42.8070N 83.7967W	no data	no data	140	8.96	778.5	535.6
OLW14	Ore Lake (north)	10/2/2021	42.48550N 83.79750W	-5.62	-41.77	164	8.8	780.6	536.5
OLW15	South Ore Creek (Brighton)	10/2/2021	42.53500N 83.7844W	no data	no data	168	8.56	649.4	449.9
OLW16	Lime Lake	10/2/2021	42.5273N 83.8119W	no data	no data	128	8.36	933.2	646.5
OLW17	Ore Lake (middle)	10/3/2016	42.48060N 83.79590W	-5.47	-40.27	no data	no data	no data	no data
OLW18	Little Ore Lake (middle)	10/3/2016	42.4742N 83.79730W	-5.5	-40.91	no data	no data	no data	no data
OLW19	Ore Lake (south)	10/3/2016	42.47600N 83.79690W	-5.65	-41.45	no data	no data	no data	no data
OLW20	Ore Lake (north)	10/3/2016	42.48570N 83.79810W	-5.56	-41.15	no data	no data	no data	no data
OLW21	East Ore Creek	10/3/2016	42.49000N 83.79100W	-6.92	-47.18	no data	no data	no data	no data
OLW22	South Ore Creek	10/3/2016	42.4977N 83.8021W	-6.45	-44.88	no data	no data	no data	no data
OLW23	Ore Lake (northwest)	2/17/2017	42.48480N 83.80150W	-7.81	-52.08	no data	no data	no data	no data

Table 1 | Chemical data for all water samples, including stable isotope data (relative to Vienna Standard Mean Ocean Water), Alkalinity (Alk.), pH, conductivity (Cond.), and total dissolved solids (TDS).

We supplement these data with historical alkalinity measurements collected by the Ore Lake Preservation Association (Fusilier, 1987, 1999) to evaluate seasonal alkalinity patterns within the lake. Figure 5 shows that Ore Lake alkalinity reaches a maxima in the spring and rapidly declines into the summer. It is likely that after reaching a late summer minima, alkalinity slowly increases throughout the fall and winter; this relationship is observed in other small lakes with abundant carbonate (Otsuki & Wetzel, 1974). This seasonal cycle probably coincides with the onset of major carbonate precipitation within the lake during the spring and summer, and reduced carbonate precipitation into the late fall and winter. No major change in lake alkalinity over time (during the 1980s, 1990s and 2020s) is observed in the summertime data. The historical alkalinity data have values that overlap and do not indicate clear change over years. Other water chemistry data (pH, conductivity, and total dissolved solids) are also reported in Table 1.

3.3. Stable isotope results

Pisoid $\delta^{18}O$ values range between -6.33 ‰ and -8.12 ‰ VPDB, with a standard deviation of 0.5 ‰. These values are broadly consistent with the bivalve shells that were sampled (mean of -6.8 ‰; Table 2). In contrast, $\delta^{13}C$ values differ considerably between pisoid and bivalve carbonate, well exceeding any potential mineralogical effect (pisoids are calcite and the shells are composed of aragonite). Pisoid $\delta^{13}C$ values range between -1.1 and -3.9 ‰ VPDB,

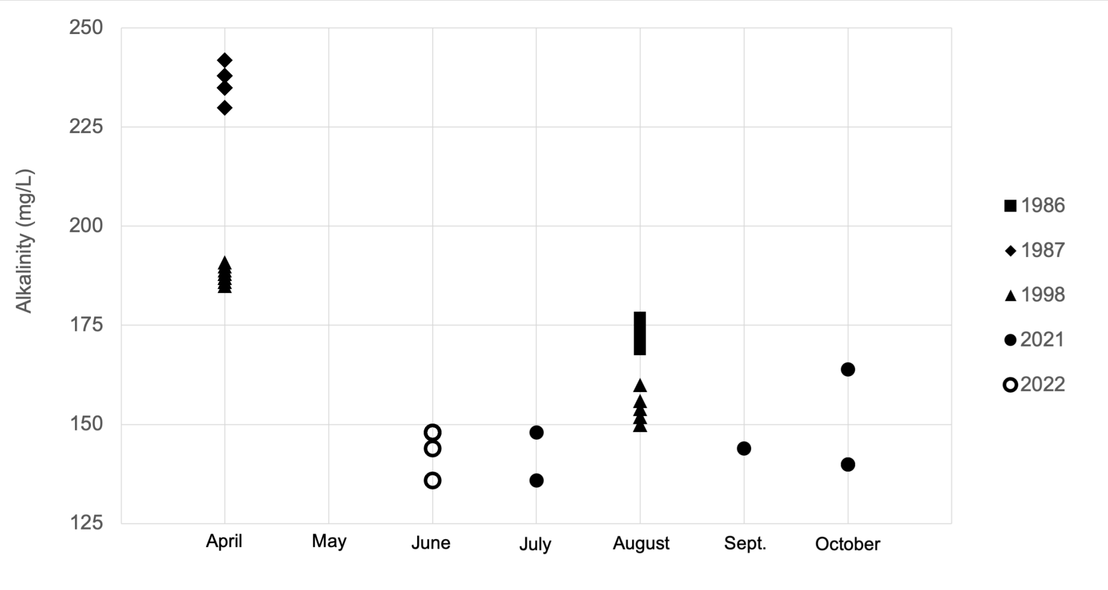

Figure 5 | Historical and recent seasonal alkalinity data from Ore Lake. We collected the 2021 and 2022 data; the older data were collected by the Ore Lake Preservation Association. Note that spring (April) data are all higher than summertime samples.

with a standard deviation of 0.6 ‰, while mollusk samples range between -5.1 and -9.1 ‰, with a standard deviation of 1.6 ‰. $\delta^{18}O$ values of water samples collected in Ore Lake during summer and fall range from -5.8 ‰ to -5.5 ‰; δD ranges from -43.6 ‰ to -40.3 ‰ (VSMOW; Table 1). A single wintertime water measurement (taken on February 17, 2017) had a $\delta^{18}O_{water}$ value of -7.8 ‰ and a δD value of -52.1 ‰ (Supplemental 3).

3.4. Formation temperature estimates from carbonate $\delta^{18}O$

Using the mean summer and fall Ore Lake $\delta^{18}O_{water}$ value of -5.6 ‰ VSMOW (see methods), calculated formation temperatures for pisoid calcite range from ~19 to ~29°C. This overlaps with the calculated temperature range for bivalve samples: ~22 to 26°C (Figure 6). Changing the estimated $\delta^{18}O_{water}$ value used for these temperature calculations results in meaningful changes. In the extreme case, using the measured wintertime $\delta^{18}O_{water}$ value of -7.8 results in a roughly 10°C decrease for all calculated temperatures. For context, annual temperatures in Ore Lake surface waters range from frozen (≤ 0°C) to approximately 27°C, with average June through August temperatures ranging from ~20 to ~27°C (Cooperative Lakes Monitoring Program, 2019; Supplemental 4).

4. Key observations and discussion

4.1. Field observations and pisoid morphology

The range of sizes of pisoids in Ore Lake is likely dependent on both the age of the pisoid and the shape of the central nucleation grain. 'Younger' (that is, smaller) pisoids that have gone through fewer cycles of summer precipitation often display different morphologies than 'older' pisoids, which have a thicker (> 5 mm) build-up of carbonate due to more (and perhaps multiple seasons of) precipitation. 'Younger' pisoids may display a shape and size that reflects a gastropod shell nucleus (asymmetric) or may reflect a smaller grained nucleus (more symmetric) (Figure 7). 'Older' pisoids fairly consistently show a subspherical morphology regardless of nucleus type.

Jones & Wilkinson (1978) suggested that turnover of pisoids in Ore Lake is minimal based on an observed 'flattening' of their structures, resulting in slightly asymmetrical banding when viewed in cross section. They suggest this occurs due to consistent contact with the substrate on one side of the pisoid, with slightly more precipitation occurring on all other surfaces (see figure 3 in Jones & Wilkinson, 1978). This interpreted lack of turnover has subsequently been cited as evidence of in-place growth of other sub-spherical carbonate structures (Riding, 1983). In contrast, Casanova (1986) found that the spherical to subspherical morphology of lacustrine concentrically laminated carbonate grains (in that case, described as oncoids) did require continuous displacement to result in similar morphology. Casanova (1986) described consistently rounded and mobile grains in the absence of turbulent waters, although the amount of transportation necessary to cause a subspherical morphology differs depending on factors including grain size and precipitation rate. We suggest that the subspherical geometry of Ore Lake pisoids is also due, at least in part, to growth during transport through the lake. This idea is supported by the existence of large shallow flats throughout the lake that would presumably provide ample area above storm wave base. Pisoid movement during growth is also consistent with field observations of complete pisoids along the lake's northern and eastern shallows (Figure 1), as well as buildup of a spit at the southern outflow made primarily of pisoid grains (Figure 4).

Water flow through Ore Lake into its southern outlet is considerable. United States Geological Survey (USGS)

N	Sample Description	$\delta^{13}C$ (VPDB)	$\delta^{18}O$ (VPDB)
1	South Pisolite 1 subsample A	-3.6	-7.2
2	South Pisolite 1 subsample B	-2.9	-6.6
3	South Pisolite 1 subsample C	-3.2	-7.3
4	South Pisolite 1 subsample D	-3.8	-7.5
5	South Pisolite 1 subsample	-2.9	-7.1
6	North Pisolite 1 subsample A	-3.3	-7.6
7	North Pisolite 1 subsample B	-3.3	-8.1
8	North Pisolite 1 subsample C	-3.5	-7.5
9	North Pisolite 1 subsample D	-3.5	-8
10	North Pisolite 2	-2.1	-7.3
11	South Pisolite 2	-3.1	-7.8
12	South Pisolite 3	-2.9	-7.7
13	South Pisolite 4	-3.9	-7.4
14	South Pisolite 5	-3.3	-7
15	South Pisolite 6	-3.3	-8
16	South Pisolite 7	-3.5	-8.3
17	South Pisolite 8	-2.6	-7
18	South Pisolite 9	-1.1	-6.3
19	South Pisolite 10	-1.7	-6.7
20	South Pisolite 11 subsample A	-3.2	-7.9
21	South Pisolite 11 subsample B	-3.2	-8.2
22	South Pisolite 11 subsample C	-2.6	-7.6
23	South Pisolite 11 subsample D	-2.7	-7.7
24	South Pisolite 12 subsample A	-3.2	-7.8
25	South Pisolite 12 subsample B	-3	-8.1
26	South Pisolite 12 subsample C	-2.4	-7.8
27	South Pisolite 12 subsample D	-2.9	-8
28	South Pisolite 13	-3.1	-7.7
29	South Pisolite 14	-3.2	-7.8
30	Bivalve 1 - Quagga Mussel	-9.1	-6.4
31	Bivalve 2 - Asian Clam	-8.4	-7
32	Bivalve 3 - Quagga Mussel	-5.1	-7.2
33	Bivalve 4 - Quagga Mussel	-9.1	-6.5

Table 2 | Stable isotope data for carbonate samples. Both $\delta^{13}C$ and $\delta^{18}O$ are measured relative to the Vienna Pee Dee Belemnite standard.

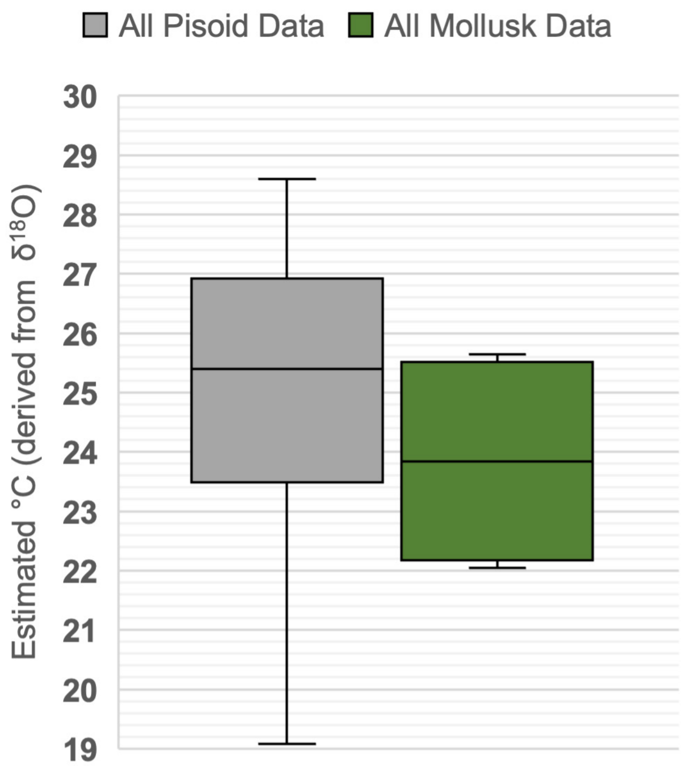

Figure 6 | Standard boxplots of temperatures calculated from carbonate $\delta^{18}O$ values using the mean of Ore Lake $\delta^{18}O_{water}$ values (-5.62 ‰ VSMOW, see text). Boxes describe the first and third quartiles of the data, and the horizontal line indicates the median. Both pisoids and local mollusks (quagga mussels and Asian clams) form in summertime temperatures.

stream gauge measurements from 2015 show that the streamflow at the southern end of the lake ranges from 0.35 m^3/s to 0.85 m^3/s, with moderate suspended debris recorded at the gauge location during high flow times (USGS, 2015). The majority of pisoids observed on the spit are complete, many of which are > 3 cm. Pisoid fragments and coarse sand is also present, along with very common disarticulated *Corbicula* sp. and *Dreissena* sp. shells. This deposition of complete and fragmented pisoids over a ~600 m^2 subaerially exposed area shows that transportation certainly takes place, and also that higher-energy storm events play some role in their movement. The only question is whether precipitation and growth occurs at times during this transport.

Pisoid growth during transport is further supported by the generally symmetrical internal laminae and overall shapes of individual pisoids we observed. This is in contrast to the argument by Jones & Wilkinson (1978) for largely immobile pisoids based on observation of consistent asymmetrical shapes, with one side flattened and the opposite side convex, which is visible both on the outermost layer (surface) and within internal laminae. However, we did not find in our samples from Ore Lake that most pisoids today have the distinctly asymmetrical structure they describe. Instead, we observed that only ~29 % of pisoid samples (20 out of 70 samples) display any notably flattened bases, where we define a flattened pisoid as having an asymmetrical geometry with one convex surface opposing a more planar surface. This suggests that most pisoids rotate sufficiently for approximately symmetrical growth. Symmetric internal laminae of most pisoids further supports this conclusion (e.g., Figure 3).

Even the minority of pisoids that do have a flatter side may have experienced transport during growth. As noted by Jones & Wilkinson (1978), the question of how cyanobacteria continue photosynthesis on the surface of the pisoid that remains in contact with the substrate – in which carbonate is precipitated in darkness to create a flattened base – remains largely unanswered. Jones &

Figure 7 | Gastropod shell grains in various stages of being coated by calcite precipitation.

Wilkinson (1978) suggest several possibilities: a) bacterial tolerance to dim light conditions, b) photosynthesis continuing via reflected light, and/or c) the transfer of nutrients via interconnected filaments. Indeed, Braissant et al. (2003) showed that dormant cyanobacterial filaments can trigger carbonate precipitation via extracellular polymeric substances and amino acids in the absence of living cyanobacteria. This may occur in Ore Lake, but it is also possible that these occasional flat sides are instead simply consistent with turnover and transportation of pisoids. Certainly, if transport is occasional and irregular, it would be expected that non-symmetrical precipitation would occur as precipitation slows on the buried side. Given that most pisoids are relatively symmetrical, regular transport of most grains likely occurred. This is further supported by thin section observations described in the below section.

4.2. Thin section and microstructure interpretations

Banding, including concentric banding, within carbonate structures is common and often interpreted as indicating seasonal or annual cyclicity (Dahanayake, 1983; Cassanova, 1986), varying biotic/abiotic influences (Richter & Sedat, 1983), and/or variable precipitation rates (Noiriel et al., 2012). Pisoids in Ore Lake display concentric banding of both porous and dense laminae that were suggested by Jones & Wilkinson (1978) to represent photosynthesis-induced precipitation (rapid and porous) that forms during the summer, and abiotic precipitation in the fall and winter (slow and relatively dense). This interpretation is based on numerous cyanobacterial filaments seen within the porous layers and the lack thereof in the denser layers. We do agree that pisoid thin sections reveal that the more porous layers seem to include more apparent cyanobacterial structures. However, instead of wintertime precipitation, we suggest that the change in the porosity of lamina within Ore Lake pisoids is a result of a changing calcite precipitation rate throughout the spring and summer seasons, and that it is therefore likely that all precipitation is influenced by microbially-induced photosynthetic effects.

In general, the porosity of modern microbial carbonates is controlled by the amount of precipitation in and around cyanobacterial filaments (Wu et al., 2021). Wu et al. (2021) found that more rapid precipitation around cyanobacterial filaments can create calcite 'crusts' (precipitation in contact with filaments), with the decay of organic matter creating porosity in-between via voids, and eventually 'mold holes'. In contrast, 'inter-crustal' precipitation (precipitation in contact with previously formed calcite) occurs when precipitation slows and results in a denser fabric (Wu et al., 2021). This conceptual framework is consistent with Ore Lake pisoid observations in this study. The lighter, more porous layers show more cyanobacterial structures in thin section (Figure 8) and likely result from calcite crust formation. The faster growth of the more porous layer is further supported by the larger (~ 0.1 mm wide) calcite crystals found occasionally within the layer (Figure 8). These are notably less common in the denser laminae and are consistent with more rapid crystal nucleation and growth (Barth & Chafetz, 2015), as is expected in the higher alkalinity conditions of the early spring and summer months (Figure 5). The darker, less porous layers likely result from slower precipitation and associated inter-crustal precipitation.

Importantly, at the thin section scale we observe generally gradual changes from the more porous to more dense layers. For instance, Figure 8B shows a fan-shaped cyanobacterial growth within the matrix of a pisoid sample. The apex of this mass shows colonization within the porous layer, and an outward growth into the dense layer. Such overlapping of laminae shows that growth is relatively continuous across the boundary. It also indicates that microbial precipitation can be ongoing while a denser lamina forms. We therefore interpret both porous and relatively dense layers to be influenced by microbial communities (i.e., both are 'biotic' precipitation), with the change in the porosity resulting primarily from a shift in the precipitation rate.

In contrast to these gradual transitions from more porous layers to more dense layers, the transition from a dense layer to a more porous layer is typically more distinct, with no observed features clearly extending across these boundaries. We therefore interpret these seemingly more abrupt shifts as a temporary cessation of precipitation. In summary, the gradual shift from porous (light) to dense (dark) laminae in Ore Lake pisoids likely represents a slowing precipitation rate as carbonate saturation in the lake water, and the amount of photosynthetic activity decreasing throughout the summer, until the end of

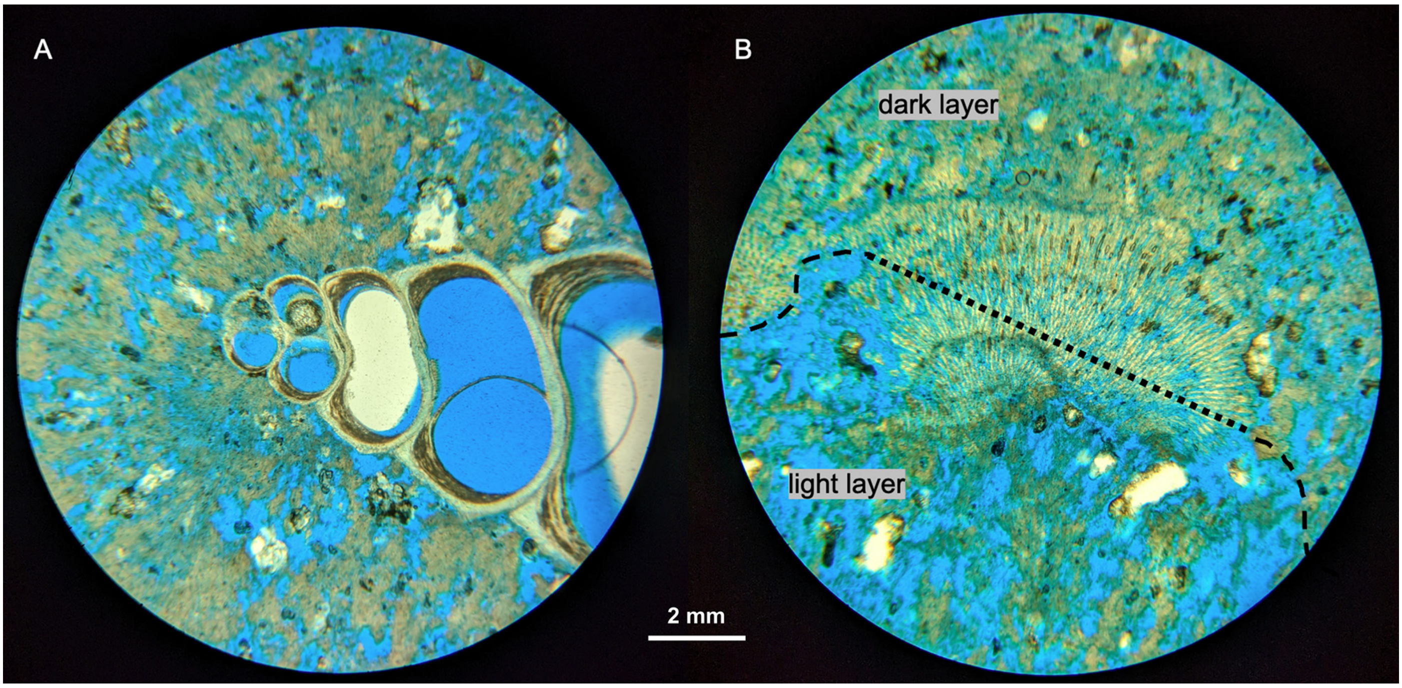

Figure 8 | Thin section images of a pisoid at 40x magnification. Slides are impregnated with blue dye indicating pore space. A: initial layering nucleating on a gastropod shell. B: Algal filaments are observed to be growing across an apparent light/dark boundary, implying continuous growth.

precipitation in fall. A new more porous layer rapidly precipitates during the following spring, coinciding with revived photosynthetic activity. This model is further supported by the isotopic results, as discussed in the next section.

4.3. Stable Isotope interpretations

4.3.1. Carbon isotopes

Carbon isotope ($\delta^{13}C$) values show large variability across sample types, with mollusks as isotopically light as -9.1 ‰ VPDB, and pisoids as isotopically heavy as -1.1 ‰ VPDB (Figure 9). The average pisoid $\delta^{13}C$ value of -3 ‰ is markedly more positive than all mollusk values, with three out of the four mollusk shells measured having $\delta^{13}C$ values lighter than -8 ‰. This large difference in $\delta^{13}C$ values reflects important differences in how carbon is incorporated into these carbonates. Importantly, bivalve shell $\delta^{13}C$ is thought to typically precipitate within a few ‰ of ambient dissolved inorganic carbon (DIC; McConnaughey & Gillikin, 2008). Although our study lacks water DIC $\delta^{13}C$ measurements, the presumed approximate $\delta^{13}C$ equilibrium of bivalve shells enables their use as a proxy for lake water DIC $\delta^{13}C$. Therefore, the positive shift in pisoid $\delta^{13}C$ of as much as ~6 ‰, relative to mollusk $\delta^{13}C$, indicates a pisoid-specific carbon isotope fractionation produced during their formation.

The significant $\delta^{13}C$ variability across pisoid samples of ~3 ‰ could have many causes. As shown in Figure 10B, $\delta^{13}C$ variability within single pisoid is smaller, averaging ~0.6 ‰. This minor variability could plausibly in-part be due to variable amounts of organic decomposition within the pisoids. The larger $\delta^{13}C$ range observed across samples is likely to be related to highly localized effects within the lake. These could include the amount of photosynthetic activity, variation in the rate of carbonate precipitation, and/or perhaps spatial differences in alkalinity (sensu Chagas et al., 2016). Importantly, despite this inherent variability, none of the pisoid measurements overlap with shell values. At the very least this several permil difference in $\delta^{13}C$ highlights that the two carbonate types are precipitated in ways that fractionate carbon isotopes quite differently.

Recent work has shown that microbialite $\delta^{13}C$ values can reflect different factors in different fresh waters, including abiotic lake DIC values (Beeler et al., 2020), sediment type and microbial diversity (Ingalls et al., 2020), mixing of water sources (e.g., thermal and fresh water; Lencina et al., 2023), and carbonate dissolution paired with photosynthesis (Wang et al., 2022). The particular $\delta^{13}C$ value of a given microbialite reflects a combination of lake water chemistry (especially Ca/Alk ratios) and biological effects such as photosynthesis (Chagas et al., 2016; McConnaughey, 1989).

Our somewhat limited view of the Ore Lake carbon system (lacking direct lake DIC measurements) inhibits our ability to attribute all the carbonate $\delta^{13}C$ variations we observed to specific factors. However, when interpreting the bivalve $\delta^{13}C$ data as an approximation of Ore Lake DIC $\delta^{13}C$, we observe a large positive fractionation that is consistent with photosynthetic effects. Preferential incorporation of ^{12}C in organic material is expected during photosynthesis (e.g., McConnaughey, 1989), thereby resulting in higher $\delta^{13}C$ values in carbonate formed in association with cyanobacteria (in this case carbonates formed in the pisoids). This interpretation supports our assertion that pisoid

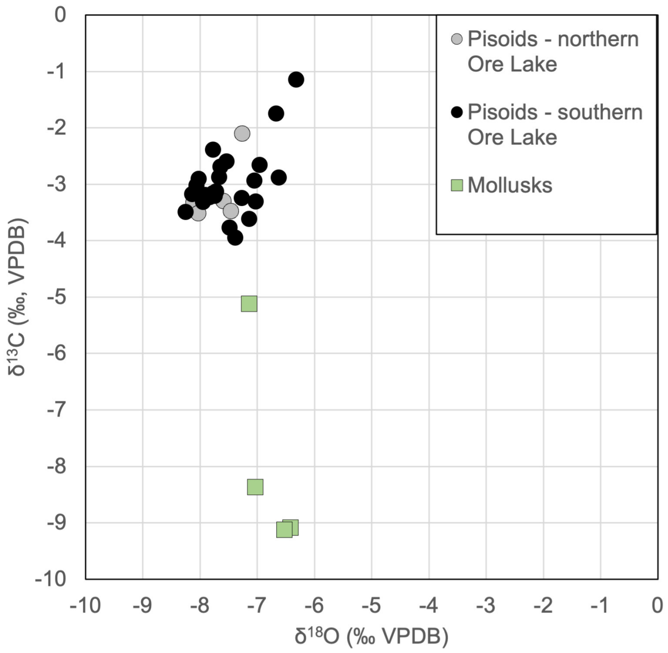

Figure 9 | Carbon and oxygen stable isotope data for all samples. No difference was observed between pisoids collected at or near the southern spit deposit (black circles) and those collected elsewhere (grey circles). Bivalve values (green squares) are overlapped by pisoid $\delta^{18}O$ values entirely, but have very different $\delta^{13}C$ values likely due to photosynthetic effects. Error bars (~0.1‰) are smaller than points.

growth does not occur abiotically in significant amounts, as all pisoid $\delta^{13}C$ measurements are consistent with photosynthetic processes. Similar magnitudes of positive $\delta^{13}C$enrichment relative to lake DIC have been observed in other examples of studies photosynthetic microbial carbonate formation (e.g., Cangemi et al., 2016). These data are also consistent with regular transport, in that precipitation is likely to have occurred primarily on light-exposed sides. Indeed, the lack of differentiation between isotopic values (both $\delta^{13}C$ and $\delta^{18}O$) for pisoids collected in different parts of the lake (Figure 9) further suggests that grains are transported during growth, as opposed to forming in discrete, stationary microenvironments.

4.3.2. Oxygen isotopes, temperature, and timing of formation

In contrast to the carbon isotope data, $\delta^{18}O$ values for Ore Lake mollusks and pisoids conform, with mollusk data (-7.2 to -6.4 ‰ VPDB) fitting entirely within the pisoid range (-8.3 to -6.3 ‰ VPDB). Although the average shell aragonite $\delta^{18}O$ value (-6.8 ± 0.3 ‰) is more positive than the average pisoid calcite $\delta^{18}O$ value (-7.5 ± 0.5 ‰), this discrepancy can be largely explained by mineralogical differences. In 25°C water for example, calcite $\delta^{18}O$ is expected to be approximately 0.5 ‰ lighter than aragonite (Grossman & Ku, 1986; Kim & O'Neil, 1997). If we make the reasonable assumption that mollusk values reflect approximate oxygen isotopic equilibrium (Wannamaker et al., 2006), then the pisoids must also reflect equilibrium conditions. These data further imply that shell and pisoid carbonate growth occur under very similar temperatures and $\delta^{18}O_{water}$ conditions, and therefore at similar times of year (Figure 6).

Indeed, temperatures derived from pisoid and lake water $\delta^{18}O$ values indicate: 1) that carbonate precipitation occurs primarily within the summer months; and 2) within ~3 m of the surface. 85 % of the estimated temperatures from pisoid $\delta^{18}O$ indicate waters in excess of 22° C, and all data exceed 19°C (Figure 10A). These warm temperatures are consistent with expected surface water temperatures for an inland lake in Michigan during the summer, and align with available Ore Lake temperature data from May through September (Supplemental 4). Although winter formation of carbonate in freshwater lakes has been directly observed (e.g., Coxon & Coxon, 1994), and has been suggested as occurring in Ore Lake (Jones & Wilkinson, 1978), our data show no evidence for cold water precipitation.

The lack of major $\delta^{18}O$ variability within and between separate pisoids also strongly supports formation solely during the warm season. A small amount of apparent temperature seasonality within individual grains (2 – 5°C) is recorded in our higher resolution sampling of four pisoids (Figure 10A; if we attribute 100 % of their $\delta^{18}O$ variability to temperature change). In reality, an amount of this variation comes from $\delta^{18}O_{water}$ variability, and so ambient temperatures during porous and dense layer precipitation are remarkably constant for a given pisoid. This is consistent with growth across multiple summers and cessation during colder periods, as we suggest above. And while our warm calculated temperatures should be considered estimates, calculations using a more negative $\delta^{18}O_{water}$ value than measured at the lake in summer and fall within this study, result in non-sensical temperatures. For example, using our wintertime $\delta^{18}O_{water}$ measurement (-7.8 ‰ VSMOW) for temperature calculation with pisoid $\delta^{18}O$ values results in an average of ~14°C, which is much warmer than actual wintertime conditions (~0°C; Cooperative Lakes Monitoring Program, 2019). Ultimately, the lack of any more positive $\delta^{18}O$ outliers (indicating colder temperatures) strongly suggests that very little precipitation occurs during the winter.

To define the timing of pisoid formation in Ore Lake more precisely than simply during the warm season, we can also consider the seasonal alkalinity cycles that are linked to carbonate precipitation in the lake. Historical data from Ore Lake (Fusilier, 1987, 1999) shows an increase in alkalinity at the beginning of the spring season, and a decline during the summer months (from 242 to 169 ppm). A decrease of alkalinity in freshwater lakes generally is often due to carbonate precipitation through dissolved CO2 loss to the atmosphere and photosynthetic processes by aquatic organisms (López-García et al., 2005). Carbonate saturation then begins to increase within the lake water during the fall and winter months, as photosynthetic organisms decrease and winter stratification begins. Müller et al. (2003) found that the total loss of inorganic carbon within

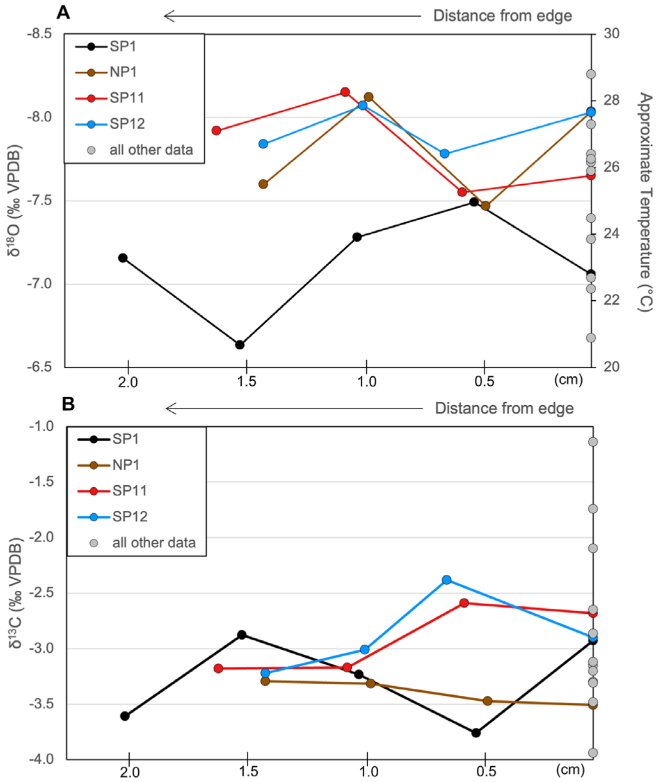

Figure 10 | Higher resolution stable isotope data taken across 4-5 layers from four pisoid samples. A: $\delta^{18}O$ data, with conversion to temperature as described in the text. Whilst all temperatures imply warm season precipitation, minor fluctuations may indicate inter-annual variability. B: $\delta^{13}C$ data that also suggests inter-annual variability, particularly in the largest sample (SP1).

lakes with a high dissolved mineral content is directly proportional to the amount of calcite precipitated, further connecting a decrease in alkalinity during the summer months to increased calcite precipitation. Considering both the known cyclical nature of alkalinity within inland lakes, and the $\delta^{18}O$ results, we suggest that the timing of formation of pisoids in Ore Lake is from late spring (late May) through the summer, and perhaps through and into September. Because of the carbonate and bicarbonate depletion during the summer, we posit that the lower temperatures observed (~19 – 23°C) may represent late spring precipitation when alkalinity first declines.

4.4. Proposed model of pisoid formation in Ore Lake

Below we suggest a model for Ore Lake pisoid formation that is consistent with our data (Figure 11):

1. During fall and winter stratification, lake water alkalinity and carbonate saturation rebound from the summer minima, reaching maximum by spring (as in Figure 5).

2. As the temperature rises, cyanobacteria begin to populate on pisoids, shells, grains, and other debris within shallow waters, likely on the wide topographic bench on the eastern side of Ore Lake. Carbonate saturation at this time is at or near maximum. Following this, carbonate precipitation occurs readily and more rapidly. This results in a porous layer due to calcite forming crusts around cyanobacterial filaments, but little inter-crustal precipitation occurs. This rapid precipitation also results in the larger calcite crystals observed within this layer.

3. As cyanobacteria continue to increase in population, the saturation decreases as carbonate continues to precipitate, with continued growth on pisoids being increasingly dependent on photosynthetic effects in the micro-environment immediately around the grain. An overall decrease in carbonate saturation thus decreases the precipitation rate of calcite crusts around cyanobacterial filaments. This slower precipitation rate allows more time for inter-crustal precipitation to occur, beginning the transition of from the formation of porous layers to the formation of dense layers.

4. By the end of summer, some precipitation still occurs, but it has been significantly reduced due to both carbonate saturation and the amount of photosynthesis beginning to decrease towards autumn. Any precipitation occurring is likely inter-crustal, which continues to create the dense layers of the pisoid. By the autumn and winter, many cyanobacterial filaments that are not encrusted in calcite begin to decay, which results in an increase in porosity.

5. Throughout the year, the flow in Ore Lake and storm events cause pisoids to be relatively consistently transported throughout the lake. The rate of this is dependent on both the size of pisoid, as well as flow rate and energy within the lake basin. During spring and summer, this transportation facilitates the precipitation on most sides of most pisoids, resulting in largely symmetric and sub-spherical morphologies. Occasionally, pisoids are not transported due to their size or local effects of obstructions, creating an asymmetric layer.

6. This cycle repeats into the next spring, where the porous layer is deposited on the previous year's dense layer, creating an abrupt contact within the microstructure.

4.5. Ore Lake pisoids in context

Laminated grains with similar morphologies have been described across the geological record (e.g., Dunham, 1969; Simonson & Jarvis, 1990; James et al., 2005; Robins et al., 2015; Chafetz et al., 2018; Laita et al., 2020). The depositional environment of these grains has been interpreted in very different ways, from vadose precipitation (Dunham, 1969) to lagoonal evaporative precipitation (Simonson & Jarvis, 1993), to near-freezing ocean precipitation (James et al., 2005). Certainly, the specific details of the environment of formation in Ore Lake described here differ from many grains with similar morphology. However,

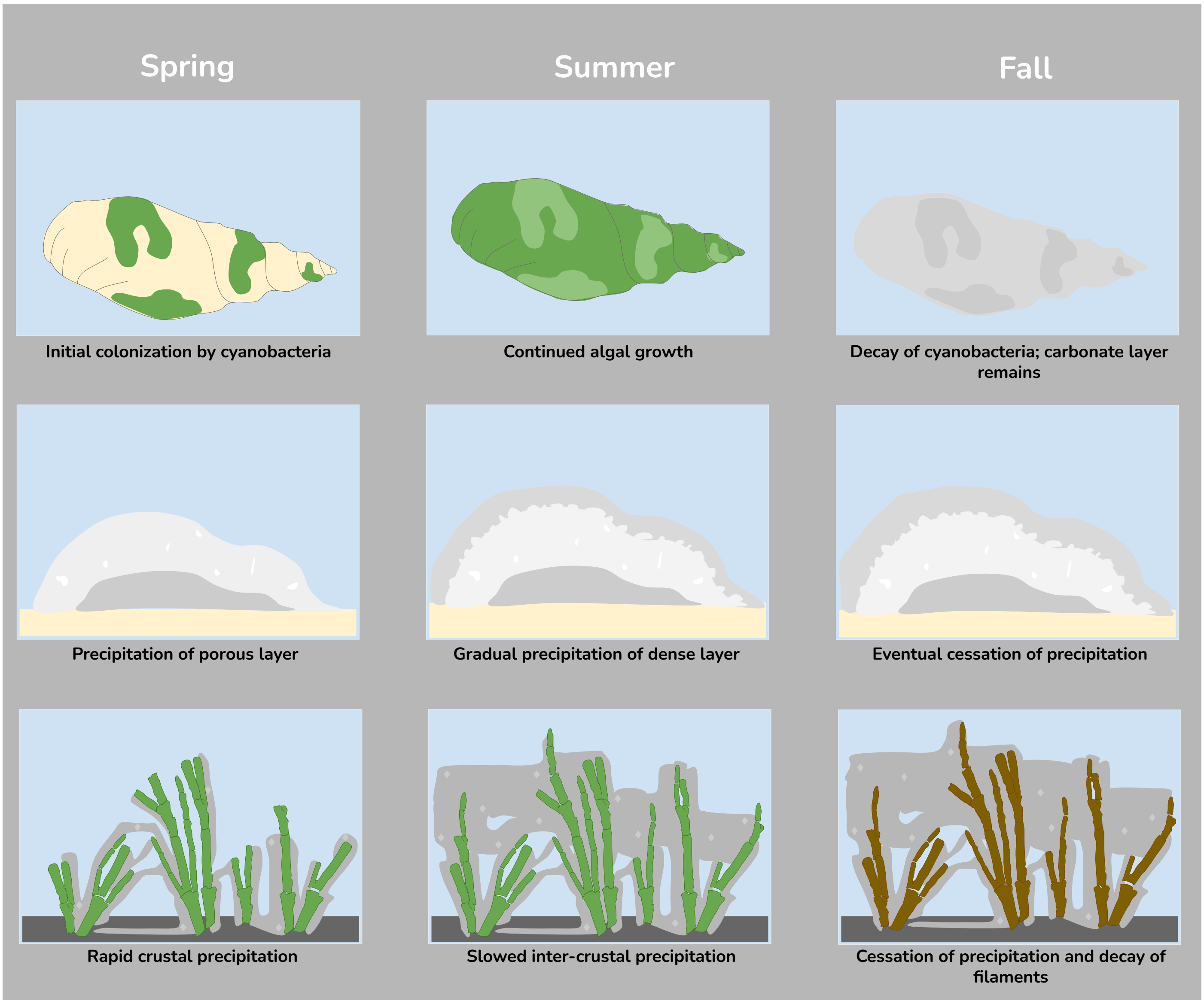

Figure 11 | A model of pisoid formation described in the text. Briefly, rapid precipitation occurs in late spring and early summer, with slower precipitation continuing throughout the warm season. Pisoid shapes imply that movement occurs throughout this time. Carbonate precipitation then ceases during the cold months.

our observations provide useful data from multiple perspectives in a modern freshwater setting. For example, our oxygen isotope data show that pisoid structures can form in approximate isotopic equilibrium with ambient waters. Indeed, it is possible that similar unaltered grains in the geological record (while rare) would accurately record past water and temperature conditions. These data also reveal that wintertime precipitation is likely insignificant in Ore Lake and therefore large temperature shifts are not required for concentric banding to form, as local biological and chemical shifts can induce these changes under consistently warm conditions. Simultaneously, our carbon isotope data strongly suggest that Ore Lake pisoid formation is facilitated by microbial photosynthetic processes. This has been similarly reported in other cases (Barth & Chafetz, 2015; Mors et al., 2022), and concentric precipitates likely form in many other freshwater settings, given the general abundance of microbial carbonate precipitation (e.g., Benzerara et al., 2014). The Ore Lake depositional environment can therefore serve as a key analogue and point of comparison for explaining the origin of other large concentric grains in the geological rock record.

Acknowledgments

We thank Lora Wingate, Kacey Lohmann, Suzanne Ankerstjerne, and Phoebe Aron for carrying out the stable isotope analyses. Tara Kneeshaw helped supply tools for water chemistry analyses. Funding was provided by the undergraduate Kindschi Fellowship Program at Grand Valley State University.

Authors contribution

R.L. and I.W. contributed to all aspects of this research paper, including conceptualization, methodology, data collection and analysis, writing and editing of the manuscript, and visualization of the results. Both authors have read and approved the final version of the paper.

Data availability

All quantitative data related to this study are in the manuscript or in the provided supplement as a .xlsx file.

Conflict of interest

We have no conflict of interest to disclose.

References

Andrews, J.E. (2006). Palaeoclimatic records from stable isotopes in riverine tufas: Synthesis and review. Earth-Science Reviews, 75(1-4), 85-104. https://doi.org/10.1016/j.earscirev.2005.08.002

Andrews, S., & Trewin, N. (2014). Paleoenvironmental significance of lacustrine stromatolite forms from the Middle Old Red Sandstone of the Orcadian Basin. Geological Magazine, 151(3), 414-429. https://doi.org/10.1017/S0016756813000290

Barth, J. A., & Chafetz, H. S. (2015). Cool water geyser travertine: crystal Geyser, Utah, USA. Sedimentology, 62(3), 607-620. https://doi.org/10.1111/sed.12158

Beeler, S., Gomez, F., & Bradley, A. (2020). Controls of extreme isotopic enrichment in modern microbialites and associated abiogenic carbonates. Geochimica et Cosmochimica Acta, 269, 136-149. https://doi.org/10.1016/j.gca.2019.10.022.

Benzerara, K., Skouri-Panet, F., Li, J., Férard, C., Gugger, M., Laurent, T., Couradear, E., Ragon, M., Cosmidis, J., Menguy, N., Margaret-Oliver, I., Tavera, R., Lopex-Garcia, P., & Moreira, D. (2014). Intracellular Ca-carbonate biomineralization is widespread in cyanobacteria. Proceedings of the National Academy of Sciences, 111(30), 10933-10938. https://doi.org/10.1073/pnas.1403510111

Binkley, K.L., Wilkinson, B.H., & Owen, R.M. (1980). Vadose beachrock cementation along a southeastern Michigan marl lake. Journal of Sedimentary Petrology, 50(3), 953-962. https://doi.org/10.1306/212F7B30-2B24-11D7-8648000102C1865D

Braissant, O., Cailleau, G., Dupraz, C., & Verrecchia, E. P. (2003). Bacterially induced mineralization of calcium carbonate in terrestrial environments: The role of exopolysaccharides and amino acids. Journal of Sedimentary Research, 73(3), 485-490. https://doi.org/10.1306/111302730485

Braissant, O., Decho, A.W., Dupraz, C., Glunk, C., Przekop, K.M., & Visscher, P.T. (2007). Exopolymeric substances of sulfate-reducing bacteria: Interactions with calcium at alkaline pH and implication of formation of carbonate minerals. Geobiology, 5(4), 401-411. http://doi.org/10.1111/j.1472-4669.2007.00117

Cangemi, M., Censi, P., Reimer, A., D'Alessandro, W., Hause-Reitner, D., Madonia, P., Oliveri, Y., Pecoraino, G., & Reitner, J. (2016). Carbonate precipitation in the alkaline lake Specchio di Venere and the possible role of microbial mats. Applied Geochemistry, 67, 168-176. https://doi.org/10.1016/j.apgeochem.2016.02.012

Casanova, J. (1986). East African Rift stromatolites. Geological Society, London, Special Publications, 25, 201-210. https://doi.org/10.1144/GSL.SP.1986.025.01.17

Chafetz, H., Barth, J., Cook, M., Guo, X., & Zhou, J. (2018). Origins of carbonate spherulites: Implications for Brazilian Aptian pre-salt reservoir. Sedimentary Geology, 365, 21–33. https://doi.org/10.1016/j.sedgeo.2017.12.024

Chafetz, H. S., & Meredith, J. C. (1983). Recent travertine pisoliths (Pisoids) from southeastern Idaho, U.S.A. In T. M. Peryt (eds.), Coated Grains, 450–455. https://doi.org/10.1007/978-3-642-68869-0_39

Chagas, A. A., Webb, G. E., Burne, R. V., & Southam, G. (2016). Modern lacustrine microbialites: towards a synthesis of aqueous and carbonate geochemistry and mineralogy. Earth-Science Reviews, 162, 338-363. https://doi.org/10.1016/j.earscirev.2016.09.012

Cooperative Lakes Monitoring Program (2019). Data Report for Ore Lake, Livingston County. https://micorps.net/lake-monitoring/clmp-documents/

Coxon, C.E., & Coxon, P. (1994). Carbonate deposition in turloughs (seasonal lakes) on the western limestone lowlands of Ireland. Irish Geography, 27(1), 14-27. https://doi.org/10.1080/00750779409478695

Dahanayake, K. (1977). Classification of oncoids from the Upper Jurassic carbonates of the French Jura. Sedimentary Geology, 18(4), 337-353. https://doi.org/10.1016/0037-0738(77)90058-6

Dahanayake, K. (1983). Depositional Environments of Some Upper Jurassic Oncoids. In: Peryt, T.M. (eds) Coated Grains 377-385. https://doi.org/10.1007/978-3-642-68869-0_32

Dunham, R.J. (1969). Vadose pisolite in the Capitan Reef (Permian), New Mexico and Texas. In: Friedman, G.M. Depositional Environments in Carbonate Rocks. https://doi.org/10.2110/pec.69.03.0182

Esteban, M., & Pray, L. C. (1983). Pisoids and pisolite facies (Permian), Guadalupe Mountains, New Mexico and West Texas. In: Peryt, T.M. (eds) Coated Grains. https://doi.org/10.1007/978-3-642-68869-0_43

Folk, R.L., & Chafetz, H.S. (1983). Pisoliths (pisoids) in Quaternary travertines of Tivoli, Italy. In: Peryt, T.M. (eds) Coated Grains. 474-487. https://doi.org/10.1007/978-3-642-68869-0_41

Fusilier, W.E., (1987). A water quality study of Ore Lake: located in Hamburg and Green Oak townships, Livingston County, Michigan. Ore Lake Preservation Association.

Fusilier, W.E., (1999). Ore Lake: A water quality re-study of the lake and its tributaries. Ore Lake Preservation Association.

Grossman, E.L., & Ku, T. (1986). Oxygen and carbon isotope fractionation in biogenic aragonite: Temperature effects. Chemical Geology: Isotope Geoscience Section, 59, 59-74. https://doi.org/10.1016/0168-9622(86)90057-6

Ingalls, M., Frantz, C., Snell, K., & Trower, E. (2020). Carbonate facies-specific stable isotope data record climate, hydrology, and microbial communities in Great Salt Lake, UT. Geobiology, 18, 566-593. https://doi.org/10.1111/gbi.12386

Irion, G., & Müller, G. (1968). Mineralogy, petrology and chemical composition of some calcareous tufa from the Schwäbische Alb, Germany. In: Müller, G., Friedman, G.M. (eds) Recent Developments in Carbonate Sedimentology in Central Europe. 157-171 https://doi.org/10.1007/978-3-642-88052-0_19

James, N. P., Narbonne, G. M., Dalrymple, R. W., & Kyser, T. K. (2005). Glendonites in Neoproterozoic low-latitude, interglacial, sedimentary rocks, northwest Canada: Insights into the Cryogenian ocean and Precambrian cold-water carbonates. Geology, 33(1), 9. https://doi.org/10.1130/G20938.1

Jones, F. G., & Wilkinson, B. H. (1978). Structure and growth of lacustrine pisoliths from recent Michigan marl lakes. Journal of Sedimentary Research, 48(4), 1103-1110. https://doi.org/10.1306/212F75FE-2B24-11D7-8648000102C1865D

Kim, S., & O'Neil, J.R(1997). Equilibrium and nonequlibrium oxygen isotope effects in synthetic carbonates. Geochimica et Cosmochimica Acta, 61(16), 3461-3475. https://doi.org/10.1016/S0016-7037(97)00169-5

Laita, E., Bauluz, B., Aurell, M., Badenas, B., Canudo, J. I., & Yuste, A. (2020). A change from warm/humid to cold/dry climate conditions recorded in lower Barremian clay-dominated continental successions from the SE Iberian Chain (NE Spain). Sedimentary geology, 403, 105673. https://doi.org/10.1016/j.sedgeo.2020.105673

Lencina, A., Soria, M., Colla, M., Cury, L., Farías, E., & Gomez, F. (2023). In situ growth of modern oncoids from Salado river, Salar de la Laguna Verde Complex, Argentina. Sedimentary Geology, 451. https://doi.org/10.1016/j.sedgeo.2023.106396.

López-García, P., Kazmierczak, J., Benzerara, K., Kempe, S., Guyot, F., & Moriera, D. (2005). Bacterial diversity and carbonate precipitation in the giant microbialites from the highly alkaline Lake Van, Turkey. Extremophiles, 9, 263-274. https://doi.org/10.1007/s00792-005-0457-0

Maliva, R. G., Missimer, T. M., Leo, K. C., Statom, R. A., Dupraz, C., Lynn, M., & Dickson, J. A. D. (2000). Unusual calcite stromatolites and pisoids from a landfill leachate collection system. Geology, 28(10), 931-934. https://doi.org/10.1130/0091-7613(2000)28%3C931:UCSAPF%3E2.0.CO;2

McConnaughey, T. (1989). ^{13}C and ^{18}O isotopic disequilibrium in biological carbonates: II. In vitro simulation of kinetic isotope effects. Geochimica et Cosmochimica Acta, 53, 163-171. https://doi.org/10.1016/0016-7037(89)90283-4

McConnaughey, T. A., & Gillikin, D. P. (2008). Carbon isotopes in mollusk shell carbonates. Geo-Marine Letters, 28(5–6), 287–299. https://doi.org/10.1007/s00367-008-0116-4

Merz, M.U.E. The biology of carbonate precipitation by cyanobacteria. (1992). Facies, 26, 81-101. https://doi.org/10.1007/BF02539795

Merz-Preiß, M., & Riding, R. (1999). Cyanobacterial Tufa Calcification in Two Freshwater Streams: Ambient Environment, Chemical Thresholds and Biological Processes. Sedimentary Geology, 12.6(1-4), 103-124. https://doi.org/10.1016/S0037-0738(99)00035-4

Monty, C.L., & Mas, J.R. (1981). Lower Cretaceous (Wealdian) Blue-Green Algal Deposits of the Province of Valencia, Eastern Spain. In: Monty, C. (eds) Phanerozoic Stromatolites. 85-120. https://doi.org/10.1007/978-3-642-67913-1_9

Mors, R. A., Gomez, F. J., Astini, R. A., Celestian, A. J., & Corsetti, F. A. (2022). Assessing the origin of pisoids within a travertine system in the border of Puna Plateau, Argentina. Sedimentology, 69(3), 1252-1275. https://doi.org/10.1111/sed.12946

Müller, B., Meyer, J. S., & Gächter, R. (2016). Alkalinity regulation in calcium carbonate-buffered lakes: Alkalinity regulation in calcium carbonate-buffered lakes. Limnology and Oceanography, 61(1), 341–352. https://doi.org/10.1002/lno.10213

Müller, B., Wang, Y., Dittrich, M., & Wehrli, B. (2003). Influence of organic carbon decomposition on calcite dissolution in surficial sediments of a freshwater lake. Water Research, 37(18), 4524-4532. https://doi.org/10.1016/S0043-1354(03)00381-6

Noiriel, C., Steefel, C., Yang, L., & Ajo-Franklin, J. (2012). Upscaling calcium carbonate precipitation rates from pore to continuum scale. Chemical Geology, 318(60-74). https://doi.org/10.1016/j.chemgeo.2012.05.014

Otsuki, A., & Wetzel, R. G. (1974). Calcium and total alkalinity budgets and calcium carbonate precipitation of a small hard-water lake. Archiv für Hydrobiologie, 14-30. https://doi.org/10.1127/archiv-hydrobiol/73/1974/14

Parker, A., & Kohlhepp, G. (2017). Michigan inland lake harmful algal bloom toxin study. Michigan Department of Environmental Quality Work Plan and Quality Assurance Project Plan. 1-17. https://www.michigan.gov/egle/-/media/Project/Websites/egle/Documents/Programs/WRD/SWAS/HAB/habs-qapp-2017.pdf?rev=a4dfc6fb83c74f7b917931d71bfddd9e&hash=2E7EFC298AFE93E1EA53D306C13CCF3C

Pedley, H. M. (1990). Classification and environmental models of cool freshwater tufas. Sedimentary Geology, 68(1-2), 143-154. https://doi.org/10.1016/0037-0738(90)90124-C

Pollock, J.B. (1919). Blue-Green Algae as Agents in the Deposition of Marl in Michigan Lakes. Michigan Academy of Science, Arts, and Letters 20, 247-260.

Reid, R. P., Visscher, P. T., Decho, A. W., Stolz, J. F., Bebout, B. M., Dupraz, C., Macintyre, I.G., Paerl, H.W., Picknewy, J.L., Prufert-Bebout, L., Steppe, T.F. & DesMarais, D. J. (2000). The role of microbes in accretion, lamination and early lithification of modern marine stromatolites. Nature, 406(6799), 989-992. https://doi.org/10.1038/35023158

Richter, D.K., & Sedat, R. (1983). Brackish-water oncoids composed of blue-green and red algae from a Pleistocene terrace near Corinth, Greece. In: Peryt, T.M. (eds) Coated Grains. 299-307. https://doi.org/10.1007/978-3-642-68869-0_26

Riding, R. (1983). Cyanoliths (Cyanoids): Oncoids formed by calcified cyanophytes. In: Peryt, T.M. (eds) Coated Grains. 276-283. https://doi.org/10.1007/978-3-642-68869-0_24

Risacher, F., & Eugster, H. P. (1979). Holocene pisoliths and encrustations associated with spring-fed surface pools, Pastos Grandes, Bolivia. Sedimentology, 26(2), 253–270. https://doi.org/10.1111/j.1365-3091.1979.tb00353.x

Rivera, M. J., & Sumner, D. Y. (2014). Unraveling the three-dimensional morphology of Archean microbialites. Journal of Paleontology, 88(4), 719–726. https://doi.org/10.1666/13-084

Robins, C. R., Deurlington, A., Buck, B. J., & Brock-Hon, A. L. (2015). Micromorphology and formation of pedogenic ooids in calcic soils and petrocalcic horizons. Geoderma, 251, 10-23. https://doi.org/10.1016/j.geoderma.2015.03.009

Shiraishi, F., Hanzawa, Y., Asada, J., Cury, L. F., & Bahniuk, A. M. (2022). Microbial influences on tufa deposition in a tropical climate. Sedimentary Geology, 427, 106045. https://doi.org/10.1016/j.sedgeo.2021.106045

Simonson, B. M., & Jarvis, D. G. (1993). Microfabrics of Oolites and Pisolites in the Early Precambrian Carawine Dolomite of Western Australia. In R. Rezak & D. L. Lavoie (eds.), Carbonate Microfabrics 227–237. https://doi.org/10.1007/978-1-4684-9421-1_17

Turchyn, A. V., Bradbury, H. J., Walker, K., & Sun, X. (2021). Controls on the precipitation of carbonate minerals within marine sediments. Frontiers in Earth Science, 9, 618311. https://doi.org/10.3389/feart.2021.618311

United States Geological Survey (USGS), 2015. Surface Water for Michigan: Streamflow Measurements. https://waterdata.usgs.gov/mi/nwis/measurements

Wanamaker Jr, A. D., Kreutz, K. J., Borns Jr, H. W., Introne, D. S., Feindel, S., & Barber, B. J. (2006). An aquaculture-based method for calibrated bivalve isotope paleothermometry. Geochemistry, Geophysics, Geosystems, 7(9). https://doi.org/10.1029/2005GC001189

Wang, W., Li, S., Zhong, J., Slowinski, S., Li, S., Li, C., Su, J., Yi, Y., Dong, K., Xu, S., Van Cappellen, P., & Liu, C. (2022). Carbonate mineral dissolution and photosynthesis-induced precipitation regulate inorganic carbon cycling along the karst river-reservoir continuum, SW China, Journal of Hydrology, 615. https://doi.org/10.1016/j.jhydrol.2022.128621.

Wu, Y. S., Jiang, H. X., Li, Y., & Yu, G. L. (2021). Microfabric features of microbial carbonates: experimental and natural evidence of mold holes and crusts. Journal of Palaeogeography, 10(1), 1-13. https://doi.org/10.1186/s42501-021-00100-5

How to cite: Landstra, R., & Winkelstern, I. (2023). Constraining the formation conditions of modern pisoids at Ore Lake, Michigan. Sedimentologika, 1(1), 1-15. https://doi.org/10.57035/journals/sdk.2023.e11.1179